Macrophage Inflammatory Protein 3α Is Involved in the Constitutive Trafficking of Epidermal Langerhans Cells

By Anne-Sophie Charbonnier,* Norbert Kohrgruber,* Ernst Kriehuber,* Georg Stingl,* Antal Rot,‡ and Dieter Maurer*

*From the *Division of Immunology, Allergy and Infectious Diseases (DIAID), Department of Dermatology, University of Vienna Medical School, A-1090 Vienna, Austria; and the ‡Novartis Forschungsinstitut, A-1235 Vienna, Austria*

Summary

Certain types of dendritic cells (DCs) appear in inflammatory lesions of various etiologies, whereas other DCs, e.g., Langerhans cells (LCs), populate peripheral organs constitutively. Until now, the molecular mechanism behind such differential behavior has not been elucidated. Here, we show that $CD1a^+$ LC precursors respond selectively and specifically to the CC chemokine macrophage inflammatory protein (MIP)-3α. In contrast, $CD14^+$ precursors of DC and monocytes are not attracted by MIP-3α. LCs lose the migratory responsiveness to MIP-3α during their maturation, and non-LC DCs do not acquire MIP-3α sensitivity. The notion that MIP-3α may be responsible for selective LC recruitment into the epidermis is further supported by the following observations: (a) MIP-3α is expressed by keratinocytes and venular endothelial cells in clinically normal appearing human skin; (b) LCs express CC chemokine receptor (CCR)6, the sole MIP-3α receptor both in situ and in vitro; and (c) non-LC DCs that are not found in normal epidermis lack CCR6. The mature forms of LCs and non-LC DCs display comparable sensitivity for MIP-3β, a CCR7 ligand, suggesting that DC subtype–specific chemokine responses are restricted to the committed precursor stage. Although LC precursors express primarily CCR6, non-LC DC precursors display a broad chemokine receptor repertoire. These findings reflect a scenario where the differential expression of chemokine receptors by two different subpopulations of DCs determines their functional behavior. One type, the LC, responds to MIP-3α and enters skin to screen the epidermis constitutively, whereas the other type, the "inflammatory" DC, migrates in response to a wide array of different chemokines and is involved in the amplification and modulation of the inflammatory tissue response.

Key words: Langerhans cell • dendritic cell • chemokine • migration • epidermis

Dendritic cells (DCs)[1] are bone marrow–derived leukocytes with specialized antigen uptake, processing, and presentation functions (for reviews, see references 1 and 2). Under normal, noninflammatory conditions, immature DCs are found in trace quantities in parenchymatous organs and contact interfaces between the body and the environment. The main DC of the epidermis is the Langerhans cell (LC), a cell type which is anchored to neighboring epithelial cells via homotypic E-cadherin (E-cad) binding (3, 4). LCs display CD1a and exhibit typical ultrastructural features (i.e., Birbeck granules) that allow their discrimination from other members of the DC family. Apparently, the still-enigmatic LC precursor migrates to the skin in the virtual absence of inflammation-related stimuli. On the other hand, other types of DCs (e.g., peripheral blood [PB]-DCs) selectively cross activated, but not resting, endothelia (5), or emerge from transmigrated blood-derived precursors in the presence of inflammatory stimuli (6). In certain disease states, inflammation-related DC types may reach the body's outermost tissues, as evidenced by the appearance of an epidermal non-LC DC population in atopic dermatitis skin (7).

Recent attention has focused on the impact of the chemokine–chemokine receptor system on DC migration. Currently, chemokines are subdivided into four subfamilies according to the position of the first cysteine pair (CXC,

[1]*Abbreviations used in this paper:* CB, cord blood; CCR, CC chemokine receptor; CXCR, CXC chemokine receptor; DC, dendritic cell; DMEC, dermal microvascular EC; EC, endothelial cell; E-cad, E-cadherin; HPC, hematopoietic precursor cell; HUVEC, human umbilical vein EC; LC, Langerhans cell; MCP, monocyte chemotactic protein; mdDC, monocyte-derived DC; MIP, macrophage inflammatory protein; MNC, mononuclear cell; PB, peripheral blood; PerCP, peridinin chlorophyll protein; PFA, paraformaldehyde; RANTES, regulated upon activation, normal T cell expressed and secreted; RPE, R-phycoerythrin; RT, reverse transcription; SA-Cy5, Cy5 RPE–conjugated streptavidin; SDF, stromal cell–derived factor; SLC, secondary lymphoid tissue chemokine.

 J. Exp. Med. © The Rockefeller University Press • 0022-1007/99/12/1755/13 $5.00
Volume 190, Number 12, December 20, 1999 1755–1767
http://www.jem.org

CC), the lack of the second and the fourth cysteine (C), or the presence of three spacing amino acids in the first cysteine tandem (CX_3Cs; for reviews, see references 8 and 9). Until now, five and nine receptors have been identified for CXC and CC chemokines, respectively. Monocyte-derived (md)DCs display migratory responsiveness to a broad array of inflammatory CC chemokines, including monocyte chemotactic protein (MCP)-1, MCP-2, and MCP-4; regulated upon activation, normal T cell expressed and secreted (RANTES), macrophage inflammatory protein (MIP)-1α, MIP-1β, and MIP-5/human CC chemokine 2 (HCC2); macrophage-derived chemokine; and the CXC chemokines IL-8 and stromal cell–derived factor (SDF)-1α (10–16). In correlation to this response profile, mdDCs express CC chemokine receptor (CCR)1, CCR2, CCR3, and CCR5, and CXC chemokine receptor (CXCR)1 and CXCR4 (10, 12, 14, 16). Interestingly, DCs generated in vitro from $CD34^+$ stem cells, but not mdDCs, express CCR6 and migrate in response to MIP-3α/liver and activation-regulated chemokine (LARC [17, 18]). During terminal maturation, mdDCs and $CD34^+$ hematopoietic precursor cell (HPC)-derived DCs acquire responsiveness to MIP-3β/EBV-induced molecule 1 ligand chemokine (ELC) because of the de novo expression of CCR7, a specific receptor for MIP-3β and secondary lymphoid tissue chemokine (SLC [10, 13, 18–21]). In keeping with an important role of CCR7 signaling for the proper function of mature DCs in vivo is the observation that *plt* mice, which lack expression of SLC, have reduced numbers of mature DCs in T cell areas of lymph nodes but, importantly, display an epidermal LC population that is normal in terms of cell numbers and distribution (22).

Based on the above considerations, we asked whether signals governing constitutive DC trafficking are at least partly different from those regulating the influx of DCs into inflammatory sites. To this end, we analyzed the chemokine responsiveness of in vitro–generated LCs and non-LC DCs, as well as of their $CD1a^+$ and $CD14^+$ precursors. Furthermore, comparative studies on the chemokine receptor profile of in vitro–generated and ex vivo–isolated LCs, as well as of inflammation-related DCs (i.e., PB-DCs), and the analysis of chemokine expression in normal human skin provided insight into the molecular interactions involved in LC homing.

Materials and Methods

mAbs and Recombinant Growth Factors and Chemokines. FITC-conjugated mAbs used were anti-CD1a, anti-CCR5, and anti–B7-2 (PharMingen); anti-CD2 and anti-CD11b (Becton Dickinson); and anti-CD3 (Immunotech). PE-conjugated mAbs included anti-CD14 (Becton Dickinson), anti-CD1a and anti-CXCR4 (PharMingen), and anti-CCR2 and anti-CCR6 (R&D Systems). The peridinin chlorophyll protein (PerCP)-conjugated anti-CD34 and anti-CD3 mAbs were from Becton Dickinson, and anti-CD1a CyChrome was from PharMingen. Biotin-conjugated anti-CCR1 was from R&D Systems. The anti–E-cad mAb (Immunotech) was biotinylated according to standard protocols. The binding of biotinylated mAbs was revealed either by PE- (Becton Dickinson) or Cy5 R-phycoerythrin (RPE)–conjugated streptavidin (SA-Cy5; Dako). Isotype control mAbs included biotinylated, FITC-, PE-, or PerCP-labeled mouse IgG1 or IgG2a (Becton Dickinson). Recombinant human (rh)GM-CSF and IL-4 were from Novartis Forschungsinstitut. rhTNF-α and rhFlt3-ligand (Flt3-L) were obtained from Genzyme and Serotec, respectively. rhMIP-1α, MIP-3α, MIP-3β, SDF-1α, RANTES, and MCP-1 were obtained from R&D Systems.

Isolation of $CD34^+$ HPCs. Cord blood (CB) was obtained according to institutional guidelines. $CD34^+$ cells were separated from CB-MNCs by a positive immunoselection procedure (CD34 MultiSort Kit; Miltenyi Biotec). In brief, CB mononuclear cells (MNCs [$1–2 \times 10^8$]) were incubated with anti-CD34 mAb–coated paramagnetic microbeads for 30 min at 4°C. After several washings, bead-bound $CD34^+$ HPCs were isolated on MiniMACS separation columns using a magnet (MiniMACS; Miltenyi Biotec). $CD34^+$ cells ($0.5–1.5 \times 10^6$) were recovered at a purity of >95%, as determined by immunostaining with a PerCP-labeled anti-CD34 mAb (clone HPCA-2) recognizing a CD34 epitope distinct from that bound by the mAb used for immunoselection.

In Vitro Generation of DCs from $CD34^+$ HPCs and Isolation of DC Precursors. $CD34^+$ HPCs were cultured in RPMI 1640 medium containing 10% FCS (both from GIBCO BRL) supplemented with 200 U/ml GM-CSF, 50 U/ml TNF-α, and 50 ng/ml Flt3-L. $CD34^+$ HPCs were cultured in 75-cm^2 tissue culture flasks (Costar) at a density of $1–2 \times 10^4$/ml. At day 3 or 4, cell suspensions were split and diluted in fresh RPMI/10% FCS supplemented with GM-CSF and TNF-α. At day 10, cells were collected and resuspended in fresh cytokine-conditioned medium at a density of $1–2 \times 10^5$/ml, and further cultured until days 12 and/or 14. Where indicated, cells were harvested at day 6 and labeled with anti-CD1a–FITC and anti-CD14–PE. $CD1a^+CD14^-$ cells ($24.6 \pm 2.0\%$ of the total population, mean ± SEM, $n = 20$) and $CD1a^-CD14^+$ cells ($36.1 \pm 2.2\%$) were isolated using a FACStar$^{PLUS™}$ flow cytometer (Becton Dickinson). The purity of the sorted cell populations was always >98%. Sorted cells were either used in chemotaxis assays, subjected to lysis and mRNA extraction, or further propagated in the presence of GM-CSF and TNF-α until days 12 and/or 14.

Isolation and Culture of Epidermal Cells and PB-DCs. Normal human skin was obtained from patients undergoing plastic surgery upon informed consent. Keratomed split-thickness skin was incubated in dispase (50 U/ml; Collaborative Biomedical Products) for 1 h at 37°C, or overnight at 4°C. Thereafter, epidermal sheets were peeled off and exposed to trypsin/0.05% EDTA (GIBCO BRL) containing 0.025% DNase 1 (Sigma Chemical Co.) for 15 min at 37°C, and cell suspensions were prepared by mechanical agitation. Residual aggregates and cellular debris were removed by filtering and density gradient centrifugation on Lymphoprep (Nycomed Amersham plc). For cell sorting experiments, epidermal cell suspensions were exposed to anti-CD11b/CD2–FITC, anti-CD1a–PE, and anti-CD3–PerCP. After several washings, $CD1a^+CD2^-CD3^-CD11b^-$ LCs and keratinocytes ($CD1a^-CD2^-CD3^-CD11b^-$ cells) were isolated using a FACStar$^{PLUS™}$ flow cytometer. Resulting cell populations were resorted to yield purities of >99%. In some experiments, sorted epidermal LCs or LC-enriched epidermal cell suspensions were cultured for the indicated time periods in GM-CSF (200 U/ml)– and TNF-α (50 U/ml)–conditioned RPMI 1640/10% FCS. PB-DCs were prepared as described previously (23, 24). In brief, PB-MNCs from healthy donors were prepared by density gradient centrifugation on Ficoll-Hypaque (Amersham Pharmacia Biotech) and subjected to counter current elutriation centrifugation (JE-6B elutri-

ation system; Beckman Instruments [24]). From the resulting cell population, T, B, and NK cells, HPCs, monocytes, and basophils were removed by anti-CD3/CD11b/CD16/CD19/CD34/CD56 immunolabeling and anti–mouse IgG immunomagnetic depletion (MACS; Miltenyi Biotec). PB-DC–enriched cell populations were further reacted with anti-CD11c–FITC, anti-CD13–PE, and anti-CD4–Cy5 mAbs, and $CD11c^+CD13^+CD4^+$ cells were isolated on a FACStar$^{PLUS™}$ flow cytometer. Purified $CD11c^+$ PB-DCs were seeded at a density of 0.5–1 $\times$ 10^6/ml in 96-well flat-bottomed microtiter plates (Costar) in RPMI 1640/10% AB serum supplemented with GM-CSF (1,000 U/ml) and IL-4 (800 U/ml).

Isolation and Culture of Dermal Microvascular ECs and Human Umbilical Vein ECs. Dermal microvascular ECs (DMECs) were isolated from human foreskins according to a protocol approved by the institutional ethics committee. Foreskins were cut into 1-cm^2 pieces and exposed to dispase (25 U/ml) for 20 min at 37°C. Cells recovered after gentle teasing of the tissue were resuspended in low-serum endothelial cell medium (PromoCell) and plated on dishes coated with fibronectin (1 μg/ml; Endogen, Inc.). For passaging, cells were recovered from the dishes by trypsin/0.05% EDTA treatment. Cells were used for further experiments at passage four. Human umbilical vein ECs (HUVECs) were isolated as described previously (25) and passaged in IMDM/20% FCS, streptomycin (100 μg/ml), penicillin (100 U/ml), L-glutamine (2 mM; all from GIBCO BRL), EC growth factor (50 μg/ml; Collaborative Biomedical Products), and heparin (5 U/ml; Sigma Chemical Co.). Activated DMECs and HUVECs were prepared by exposing the cells for 6 h to 50 ng/ml IFN-γ (Endogen, Inc.).

mRNA Extraction and Reverse Transcription PCR Amplification. Primary human cells isolated and cultured as described above were lysed at a cell density of 4 $\times$ 10^6/100 μl in Tris/lithium-dodecylsulfate (LiDS)-containing buffer (100 mM Tris-HCl, 500 mM LiCl, 10 mM EDTA, 1% LiDS, 5 mM dithiothreitol, pH 8.0) for 5 min at 4°C. Poly(A) RNA was isolated using oligo $(dT)_{25}$-conjugated Dynabeads (Dynal) according to the manufacturer's recommendations. In brief, 30 μl of the Dynabead oligo $(dT)_{25}$ suspension was added to 100 μl cell lysate, and beads were allowed to hybridize with mRNA poly(A) tails for 5 min at room temperature. Bead-bound poly(A) RNA was retrieved using a magnetic particle concentrator (Dynal), and mRNA was eluted for 3 min at 65°C in H_2O. Reverse transcription (RT) of purified mRNA was performed using the avian myeloblastosis virus (AMV) first strand cDNA synthesis kit (Boehringer Mannheim). In brief, eluted mRNA was incubated with 10 mM Tris-HCl, 50 mM KCl, 5 mM $MgCl_2$, 1 mM dNTP, 0.04 A_{260} U Oligo-$p(dT)_{15}$ primer, 50 U RNase inhibitor, and 20 U AMV reverse transcriptase for 1 h at 42°C. Thereafter, the reverse transcriptase was inactivated by heating the reaction mix to 99°C for 5 min. PCR amplifications were performed in 50 μl reaction buffer (20 mM $[NH_4]_2SO_4$, 75 mM Tris-HCl, pH 8.8, 0.01% Tween 20, 1.5 mM $MgCl_2$, 0.2 mM of each dNTP, and 2.5 U thermostable DNA polymerase; all from Advanced Biotechnologies Ltd.), and

Table I. *Sequences of Primers Used for PCR Amplification of cDNA Derived from Chemokine Receptor/Chemokine Transcripts, and Sizes of Products*

Transcript	Primer sequences (5′–3′)	Product size
		bp
CCR1	AAG CTT CAG AGA GAA GCC GGG ATG GAA ACT CC (ref. 46)	1,094
	CTC GAG CTG AGT CAG AAC CCA GCA GAG AGT TC (ref. 46)	
CCR2	TGG CTG TGT TTG CTT CTG TC	229
	TCT CAC TGC CCT TAT GCC TCT	
CCR3	AAG CTT CAG GGA GAA GTG AAA TGA CAA CC (ref. 46)	1,084
	CTC GAG CAG ACC TAA AAC ACA ATA GAG AGT TCC (ref. 46)	
CCR5	TTC CCC TAC AAG AAA CTC TC	328
	ATT TCC AAA GTC CCA CTG GG	
CCR6	TTT TTC TGC CCA CAA TGA GCG G	1,217
	GCA TAC CTG GCC ATA GAC TTT TTT	
CCR7	CAT GGA CCT GGG GAA ACC AA	1,174
	CTG GGA GAG GTC CCT CTA GT	
CXCR4	AAG CTT GGA GAA CCA GCG GTT ACC ATG GAG GGG ATC (ref. 46)	1,084
	CTC GAG CAT CTG TGT TAG CTG GAG TGA AAA CTT GAA GAC TC (ref. 46)	
MIP-3α	CTG TAC CAA GAG TTT GCT CC	254
	GCA CAA TAT ATT TCA CCC AAG	
MIP-3β	TGC CTG TAG TGT TCA CCA	286
	CTC ACA CTC ACA CAC ACC CC	
β-actin	ATC TGG CAC CAC ACC TTC TAC AAT GAG CTG CG*	838
	CGT CAT ACT CCT GCT TGC TGA TCC ACA TCT GC*	

ref., reference.
*Sequences from Clontech.

20 pM of each primer. Sequences of primer pairs used are given in Table I. cDNA derived from mRNA of 10^4 cells was used as template for individual PCR reactions. Amplified products were subjected to 2% agarose gel electrophoresis and visualized by ethidium bromide (Sigma Chemical Co.) staining.

Transwell Insert Chemotaxis Assay. Chemotaxis assays were performed as described previously (26). Cells, either directly recovered from cultures at the indicated days or FACS® sorted and recultured overnight in GM-CSF/TNF-α–conditioned medium, were washed and resuspended in migration buffer (HBSS [GIBCO BRL], 1 mM $CaCl_2$, 0.5 mM $MgCl_2$, 0.1% BSA [Sigma Chemical Co.)] at a density of 2–3 × 10^6 cells/ml. 600 μl of chemokine solution or buffer alone was added to individual wells of 24-well plates (Costar) on ice. Immediately thereafter, Costar transwell devices with 5-μm pore size, polyvinylpyrrolidone-free polycarbonate membranes were inserted into the wells, and 100 μl cell suspension was layered on top of the membrane. In experiments addressing directional versus random migration, different concentrations of chemokines were placed above and/or below the membrane. Cells were allowed to attach to and transmigrate through the membrane for 2 h at 37°C. The fluid phase above the membrane was then removed, transwell inserts were taken out of the wells, and membrane-bound cells were stained with Hemacolor (Merck) for enumeration, or were fixed with 4% paraformaldehyde (PFA; Fluka AG) for 30 min at 4°C, washed, and processed for confocal laser scanning analysis as described below. Non–membrane-bound, transmigrated cells were recovered by complete aspiration of the remaining solution in the well. These samples (i.e., 600 μl) were pooled with the eluates obtained after two washes of the same well with 200 μl HBSS. Complete removal of cells from the wells was checked by light microscopy. 10% of the volume (i.e., 100 μl) of individual samples was subjected to cell enumeration on a FACScan™ (Becton Dickinson). Using appropriate forward scatter threshold settings, all cells contained in individual samples were acquired. The number of cells fulfilling the same forward/side scatter criteria as the cells before migration was multiplied by 10 to reveal the absolute number of migrated cells. Cell numbers calculated by this flow cytometry measurement correlated well with those obtained by conventional trypan blue exclusion counting using a hemocytometer (data not shown). Cells recovered from the remaining 9/10 of the samples were double/triple-stained with anti-CD1a–FITC and anti-CD14–PE (cells recovered from 6-d cultures) or with anti-CD1a–FITC, anti-CD11b–PE, and biotinylated anti–E-cad/SA-Cy5 (cells recovered from 12- or 14-d cultures).

Confocal Laser Scanning Microscopy. After PFA fixation, cells bound to the transwell membrane were stained with 1 μg/ml propidium iodide in PBS/0.001% saponin (both from Sigma Chemical Co.) for 1 h at room temperature. Membranes were then cut out of the transwell inserts, mounted onto slides, and embedded in VectaShield medium (Vector Laboratories). Slides were examined using a confocal laser scanning microscope system (LSM 410; Carl Zeiss, Inc.) equipped with a laser emitting light at 488 nm. Membranes were scanned horizontally by acquiring 32 sections within a depth of 64 μm. Vertical images were obtained by three-dimensional transformation of data obtained by horizontal sectioning.

Boyden-type Microchamber Chemotaxis Assay. For comparison, cell migration was also evaluated using the microchamber chemotaxis assay (NeuroProbe) as described previously (27). Chemokines were diluted as described above, and 30 μl of chemokine solution or buffer alone was pipetted into individual wells of the 48-well bottom chamber. Wells were covered with a 5-μm pore size, polyvinylpyrrolidone-free polycarbonate membrane and a plate forming the upper compartments. 50 μl of cell suspension (10^6 cells/ml) was placed into the upper compartment of each well. Chambers were incubated for 2 h at 37°C, filters were harvested, nonmigrated cells were removed, and the migrated filter-bound cells were stained with Hemacolor. Chemokine-induced cell migration was analyzed by computer-assisted counting (Optomax V; Bestobell Mobrey) of the cells adherent to the bottom side of the membrane.

Flow Cytometry Analysis. For two- or three-color immunolabeling, cells were washed twice in ice-cold PBS and incubated in 50 μl PBS containing the appropriate biotin- and/or fluorochrome-labeled mAbs (2.5 μg/ml each) for 30 min on ice. For the detection of cell-bound biotinylated mAbs, cells were further exposed to 1 μg/ml SA-PE or SA-Cy5. At least 10,000 cells were analyzed on a FACScan™ (Becton Dickinson). For the detection of intracellular antigens, cells were subjected to fixation and permeabilization after surface immunostaining using a kit according to the manufacturer's recommendations (Fix & Perm; An der Grub Bioresearch).

Actin Polymerization. HPC-derived cells were harvested on day 6, washed, and resuspended in migration buffer (1 × 10^6 cells/ml). After allowing the cells to equilibrate for 15 min at 37°C, buffer only or MIP-1α at the indicated final concentration was added. After the indicated incubation periods, the reaction was stopped by adding PFA (final concentration 0.1%), and individual samples were incubated for 30 min at 4°C. Thereafter, cells were washed and sequentially exposed to anti-CD1a–CyChrome/anti-CD14–PE and saponin (final concentration 0.1%)/phalloidin–FITC (final dilution 1:5,000; both from Sigma Chemical Co.), and subjected to FACS® analysis.

Immunohistochemistry. Normal human skin was removed during elective plastic surgery upon informed consent. The skin samples were snap-frozen in liquid nitrogen–chilled isopentane. Frozen sections were mounted onto glass slides and fixed for 10 min in acetone at room temperature. Thereafter, the slides were kept at −20°C for up to 8 wk, until the staining procedure. For immunostaining, the slides were rehydrated and incubated with the following primary Abs: rabbit anti–MIP-3α, anti–MIP-3β (Peprotech), and anti-CCR6 (gift of Joshua Farber, National Institutes of Health, Bethesda, MD [28]); monoclonal mouse anti–HLA-DR (Biotest), mouse anti-CCR6, anti–MIP-1α, anti–MIP-1β, and anti-RANTES; and goat anti–SDF-1α and anti–MCP-1 (all from R&D Systems). The bound primary Abs were detected by sequential incubations with alkaline phosphatase–conjugated goat anti–rabbit, rabbit anti–mouse, or rabbit anti–goat secondary Abs and an alkaline phosphatase–anti-alkaline phosphatase staining kit (Dako), according to the manufacturer's instructions. To control the specificity of Ab binding, rabbit, goat, and mouse Ig and IgG control Abs (Dako) were used at equimolar concentrations. Each immunostaining protocol was performed on skin from at least three different donors.

Results and Discussion

LCs and Non-LC DC Precursors Respond to Different Sets of Chemokines. In a first series of experiments, we investigated whether chemokines can induce the migration of well-defined DC types and their precursors in a selective manner. As a model system, we used the cellular progeny of GM-CSF/TNF-α–stimulated $CD34^+$ HPCs. Under these culture conditions, virtually nonoverlapping $CD1a^+$ and $CD14^+$ cell subsets appear around day 6. Until day 12, they

develop into E-cad$^+$CD11b$^-$CD1a$^+$ LCs and E-cad$^-$ CD11b$^+$CD1a$^+$ non-LC DCs, respectively (29; data not shown). Chemokines that have been found to induce the migration of bulk DC populations of various maturational stages and lineages (i.e., MIP-1α, RANTES, MIP-3α, MIP-3β, MCP-1, and SDF-1α) were tested. Fig. 1 shows that, on the basis of their chemokine response pattern, CD1a$^+$ LCs and CD14$^+$ non-LC DC progenitors are functionally diverse cell populations. Most importantly, MIP-3α, a cytokine with chemotactic activity for CD34$^+$ HPC-derived DCs, but not mdDCs (18), attracted almost exclusively CD1a$^+$ LC precursors (Fig. 1 A). The maximal MIP-3α–induced response measured for CD14$^+$ cells and for the residual, presumably poorly differentiated, CD14$^-$ CD1a$^-$ cell population was at least threefold lower and only occurred at an MIP-3α concentration 100-fold higher than that needed to achieve a similar migratory response with CD1a$^+$ LC precursors (Fig. 1 A). We also confirmed, by a checkerboard assay, that the CD1a$^+$ LC precursors, as well the few CD14$^+$ cells that were attracted by MIP-3α, migrated in a directional rather than a random fashion (data not shown).

In addition to being a selective chemoattractant for LC precursors, MIP-3α was the only chemokine in the panel tested that induced potent and efficacious migratory responses of these cells. LC precursors responded only weakly to SDF-1α and MIP-3β (Fig. 1, C and D), and did not migrate at all in response to MCP-1, which, in contrast, attracted some CD14$^+$ non-LC DC precursors (Fig. 1 B). Another chemoattraction profile was observed for the CD14$^-$ CD1a$^-$ cell population. As seen previously with HSCs, these cells were attracted by SDF-1α (Fig. 1 C [30]) and responded to MCP-1 (Fig. 1 B), but not to MIP-3α or MIP-3β (Fig. 1, A and D). As shown in Fig. 2 A, MIP-1α failed to induce migration of day 6 CD34$^+$ HPC-derived DC precursors. The apparent lack of migratory response to this chemokine was surprising, since day 6 DC precursors express CCR1 and CCR5, both of which are receptors for MIP-1α (see below). The transwell migration assay used allows only the analysis of cells that have passed the membrane and detached into the lower chamber, whereas the cells that remain membrane bound escape detection. To control for the cells adherent to the lower side of the membrane, we also tested MIP-1α in the Boyden-type chamber assay, which detects the migrated, membrane-bound cells only. The direct comparison of the results obtained in these two migration assays, plus the analysis of the transwell mem-

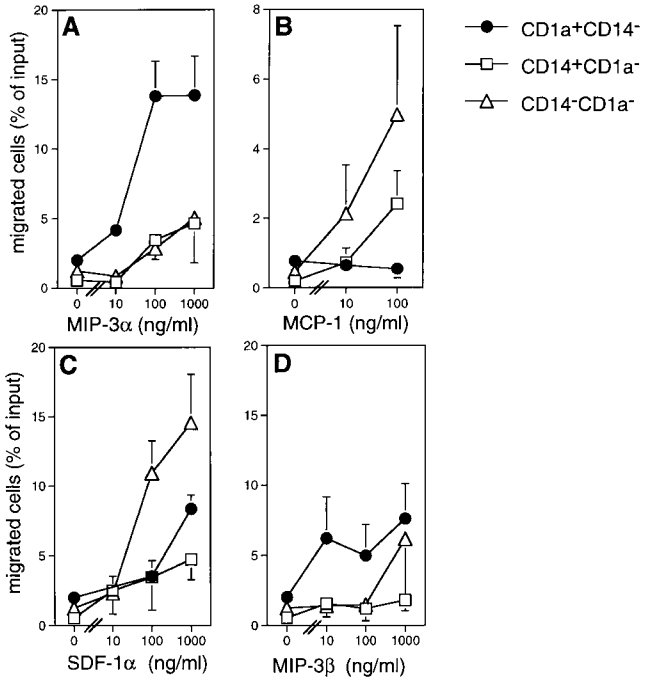

Figure 1. Chemotactic response of LC and non-LC DC precursors generated in vitro from CD34$^+$ HPCs. CB-derived HPCs were stimulated for 6 d with GM-CSF/TNF-α and then studied in the transwell chemotaxis assay. MIP-3α (A), MCP-1 (B), SDF-1α (C), or MIP-3β (D) was placed in individual wells of 24-well plates, transwell devices were inserted, and cell suspensions were layered into the transwell inserts. After 2 h at 37°C, the cells that transmigrated into the lower compartment were harvested, stained with anti-CD1a–FITC and anti-CD14–PE, and subjected to FACS® analysis. Results are given as the number of transmigrated cells in percentage of the input cell number of individual subpopulations (CD1a$^+$CD14$^-$, filled circles; CD14$^+$CD1a$^-$, open squares; CD14$^-$CD1a$^-$, open triangles). Mean ± SEM values obtained in three different experiments are shown.

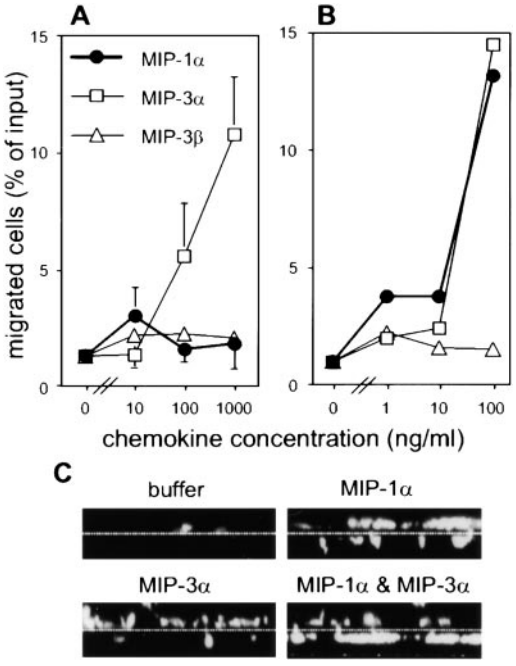

Figure 2. MIP-1α and MIP-3α elicit different migratory and/or adhesive responses in CD34$^+$ HPC-derived LC and DC precursors. Results shown in A and B were obtained using the transwell chemotaxis assay and the 48-well Boyden-type chamber chemotaxis assay, respectively. For both assays, day 6 LC and/or DC precursors were harvested and tested for their migratory responses to MIP-1α (filled circles), MIP-3α (open squares), and MIP-3β (open triangles). Mean percentages (± SEM) of migrated and detached (A; $n = 3$) and migrated, membrane-bound cells (B; $n = 2$) are shown. (C) Representative vertical sections through 5-μm pore size membranes used in the transwell chemotaxis assay. The assays were performed using the indicated stimuli (MIP-1α at 100 ng/ml, MIP-3α at 1 μg/ml, and the combination of both), or buffer alone. Membrane-bound cells were fixed and labeled, and membranes were subjected to confocal laser scanning microscopy. Broken lines denote the position of the membrane.

branes by confocal microscopy, showed that MIP-1α was eliciting migratory and/or adhesive responses in $CD34^+$ HPC-derived DC precursors that were different from those induced by MIP-3α (Fig. 2, A and B). In both the transwell and the Boyden-type assay, the cells that had been attracted by MIP-1α remained adherent to the membrane (Fig. 2, B and C). In contrast, the cells that had responded to MIP-3α detached from the lower side of the membrane in the transwell system (Fig. 2 A) and remained membrane bound only in the Boyden-type assay (Fig. 2 B). The proadhesive effect of MIP-1α was pronounced also when an additional migration-inducing stimulus (e.g., MIP-3α) was provided at the same time (Fig. 2 C).

To better characterize the cell populations that respond to chemokines by adhesion versus transmigration, $CD1a^+$ and $CD14^+$ DC precursor subsets were flow sorted on day 6, recultured overnight, and then tested in the transwell chemotaxis assay. In concordance with our results obtained with nonsorted DC precursor subsets, MIP-3a induced vigorous transmigration of sorted $CD1a^+$ LC, but not of $CD14^+$ non-LC DC precursors (Fig. 3 A). The enumeration of cells that migrated but did not detach from the transwell membranes revealed that only a minor part of the migrated $CD1a^+$ LC precursors remained membrane bound, and that only very few $CD14^+$ cells adhered to the filters in response to MIP-3α (Fig. 3 B). The argument that LC, rather than non-LC DC precursors, are the main MIP-3α–responsive cell population was further corroborated in the Boyden-type microchamber chemotaxis assay using flow-sorted $CD1a^+$ and $CD14^+$ DC precursors (data not shown). In another series of experiments, we used the same experimental set-up to study MIP-1α–induced migration of isolated DC precursors. However, unlike their nonsorted founder population, neither of the two sorted DC precursor subsets significantly migrated to MIP-1α either in the transwell or in the Boyden-type microchamber chemotaxis assay (data not shown). The reason for this discrepancy is not currently understood, but may be due to desensitization of MIP-1α receptors by chemokines (3, 4, 21) released after the sorting procedure. To still be able to identify the principal MIP-1α–responsive DC precursor, we measured MIP-1α–induced actin polymerization, a cellular event occurring early after chemokine receptor triggering (8). As revealed by filamentous (F)-actin and mAb co-staining experiments performed on nonsorted day 6 DC progenitor subsets, $CD14^+$ non-LC DC precursors and, to a lesser extent, $CD1a^-CD14^-$ cells, but no $CD1a^+$ LC precursors, responded to MIP-1α (Fig. 3 C). In summary, our cumulative data indicate that MIP-1α (Fig. 2) and RANTES (not shown), which act on the same set of receptors, induce non-LC DCs rather than LC precursors to migrate and to firmly adhere to the substratum. It is possible that the differential responses of defined DC precursors to MIP-3α and MIP-1α may be important for the fine-tuning of migration- versus adhesion-dependent immobilization and, as a result, for the correct localization of the various types of DCs in the tissues.

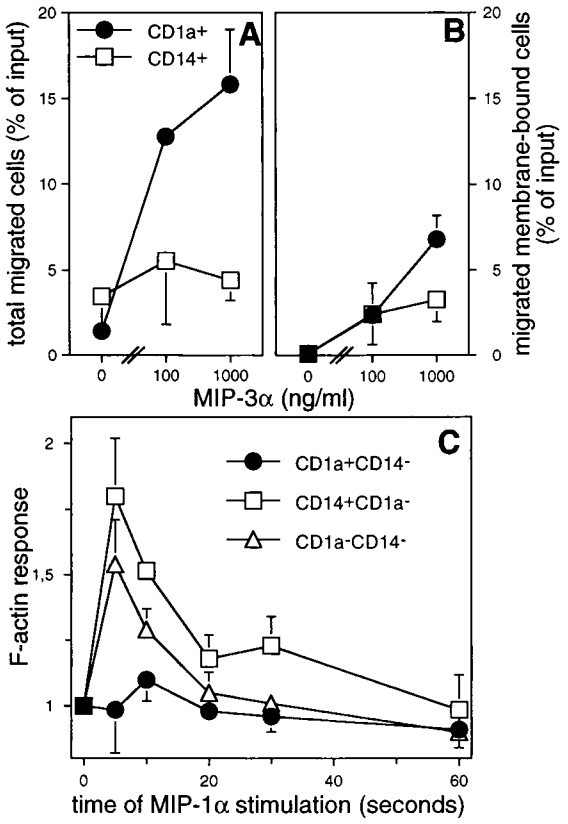

Figure 3. Differential responses of LC and non-LC DC precursors to MIP-3α and MIP-1α. (A and B) MIP-3α induces migration of LC but not non-LC DC precursors. Day 6 $CD1a^+CD14^-$ and $CD14^+CD1a^-$ DC precursors were flow sorted, recultured overnight in GM-CSF/TNF-α–supplemented medium, and thereafter subjected to the transwell chemotaxis assay. MIP-3α or buffer only was placed in individual wells of 24-well plates, transwell devices were inserted, and cell suspensions were layered into the transwell inserts. After 2 h at 37°C, migrated cells that detached into the lower compartment and migrated cells that remained membrane bound were counted. (A) Mean percentages (± SD; $n = 2$) of all migrated cells (detached plus membrane bound); (B) mean percentages (± SD; $n = 2$) of migrated, membrane-bound cells; $CD1a^+CD14^-$, filled circles; $CD14^+CD1a^-$, open squares. (C) MIP-1α mediates rapid actin polymerization in non-LC DC but not LC precursors. Cells were incubated for the indicated time periods in the presence or absence of 100 ng/ml MIP-1α. Cells were fixed with PFA, exposed to anti-CD1a–CyChrome/anti-CD14–PE, and F-actin was stained by an incubation with saponin/phalloidin–FITC. The F-actin response (y-axis) of individual cell populations is given as the ratio of the mean phalloidin-FITC fluorescence intensity in the presence of MIP-1α over the mean phalloidin-FITC fluorescence intensity in its absence. X-axis, elapsed time; $CD1a^+CD14^-$ LC precursors, filled circles; $CD14^+CD1a^-$ non-LC DC precursors, open squares; $CD1a^-CD14^-$ cells, open triangles. Mean ± SD values obtained in two different experiments.

LCs and Non-LC DCs Do Not Respond to Chemokines That Attract Their Precursors, but Both Respond to MIP-3β. When we compared the effect of chemokines on the migration of $E\text{-}cad^+CD11b^-CD1a^+$ LCs and of $E\text{-}cad^-CD11b^+CD1a^+$ non-LC DCs between days 12 and 14, we observed that neither of the DC types responded to MIP-3α (Fig. 4 A). In fact, it appears that LCs have completely lost the MIP-3α reactivity characteristic of their precursor stage, and that the non-LC DCs did not acquire responsiveness to MIP-3α. The finding of a selective but transient

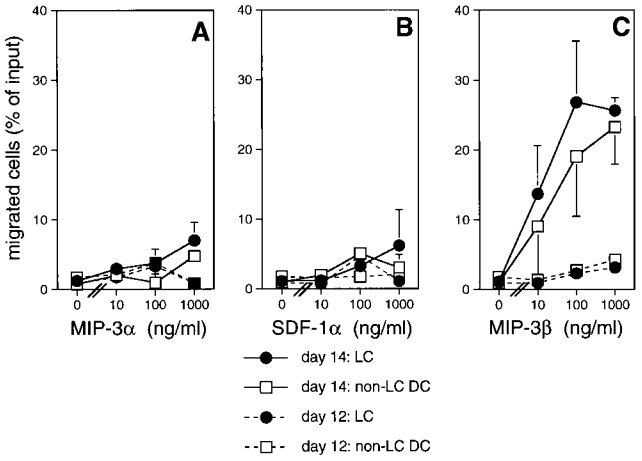

Figure 4. Chemotactic response of LCs and non-LC DCs generated in vitro from $CD34^+$ HPCs. CB-derived HPCs were stimulated for 12 or 14 d with GM-CSF/TNF-α and then studied in the transwell chemotaxis assay. MIP-3α (A), SDF-1α (B), or MIP-3β (C) was placed in individual wells of 24-well plates, transwell devices were inserted, and cell suspensions were layered into the transwell inserts. After 2 h at 37°C, the cells that transmigrated into the lower compartment were harvested and stained with anti-CD1a–FITC, anti-CD11b–PE, and biotinylated anti-E-cad, followed by SA-Cy5. Results are given as the number of transmigrated LCs and non-LC DCs in percentage of the input cell number of each DC subpopulation (LCs: E-$cad^+CD11b^-CD1a^+$, filled circles; non-LC DCs: E-$cad^-CD11b^+CD1a^+$, open squares) at day 12 (broken lines) and day 14 (solid lines). Mean ± SEM values obtained in three different experiments are shown.

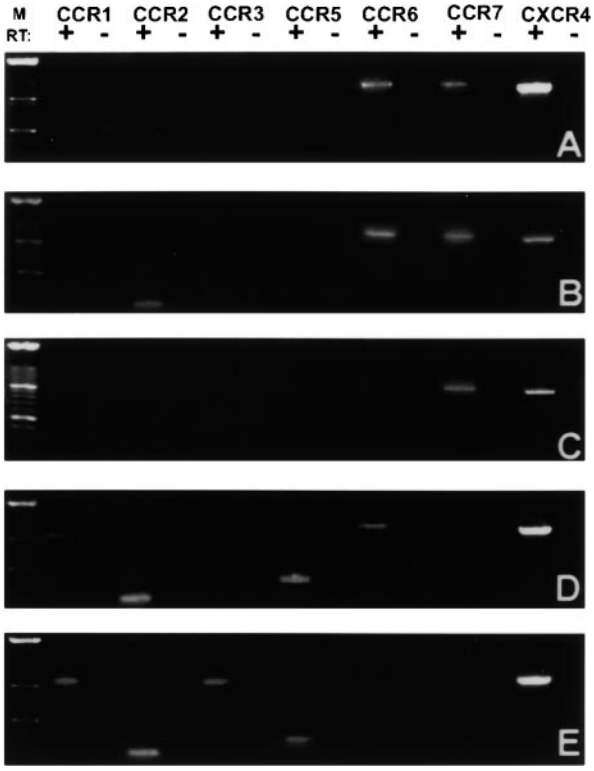

Figure 5. RT-PCR analysis of transcripts encoding chemokine receptors in different DC types generated in vitro and purified ex vivo. cDNAs from the following cell populations were prepared and subjected to PCR: (A) in vitro–generated LCs, derived from flow-sorted $CD1a^+$ LC precursors of 6-d-old $CD34^+$ HPC cultures, analyzed on day 12; (B) epidermal LCs, freshly isolated from skin and purified by FACS®; (C) flow-sorted epidermal LCs cultured for 48 h in the presence of GM-CSF/TNF-α; (D) bulk progeny of GM-CSF/TNF-α–stimulated $CD34^+$ HPCs at day 6; (E) freshly isolated $CD11c^+$ PB-DCs. RT, reverse transcription of mRNA; M, molecular size markers. For primer sequences, see Table I.

involvement of MIP-3α in the migration of defined LC precursors, but not of monocyte-related DC/DC precursors (Fig. 1 A and Fig. 4 A), together with the observation of a temporary appearance of MIP-3α–responsive cells in bulk progenies of cytokine-stimulated $CD34^+$ HPCs (18), suggests that MIP-3α could have a specific role in guiding LC precursors to their correct anatomical location in vivo. The refractory state for chemokine-induced migration seen at day 12 of the cultures (Fig. 4, A–C) lasts for only a short time period, since at day 14 the LC/DC progeny displayed pronounced migratory responses to MIP-3β (Fig. 4 C). Data presented in Fig. 4 C also show that day 14 LCs and non-LC DCs display quantitatively comparable chemotactic responses to MIP-3β. Thus, DCs show subtype-restricted chemokine responses at the committed precursor stage only.

LCs Display a Restricted Set of Chemokine Receptors. To see (a) whether a correlation exists between the chemokine expression pattern and the migratory properties of different types of DCs, and (b) whether our findings are relevant to the in vivo situation, we analyzed the chemokine receptor profile of in vitro–generated LCs and freshly isolated epidermal LCs. As shown in Fig. 5 B, epidermal LCs express mRNAs encoding CCR6, CCR7, and CXCR4, which are the receptors for MIP-3α, MIP-3β/SLC, and SDF-1, respectively. In contrast, these cells are virtually devoid of CCR1, CCR3, and CCR5 transcripts, and express only limited amounts of CCR2 mRNA. Although a similarly restricted set of chemokine receptor mRNAs was expressed by in vitro–generated LCs (Fig. 5 A), other types of immature DCs and DC precursors, i.e., the progeny of cytokine-stimulated $CD34^+$ HPCs at day 6 (Fig. 5 D), blood DCs (Fig. 5 E), and monocyte and/or mdDCs (10, 13, 31), express mRNA for a wide array of different chemokine receptors, including CCR1, CCR2, CCR3, CCR5, and CXCR4. These two different patterns were mirrored by the FACS® data of chemokine receptor expression on the surface of in vitro–generated LC versus non-LC DC precursors (Fig. 6 A). CCR6 was the only chemokine receptor among those studied that was present on the surface of $CD1a^+$ LC precursors (Fig. 6 A). Curiously, CXCR4 was not detected on the surface of these cells, but was found in their cytoplasm (Fig. 6 A; data not shown). In contrast, $CD14^+$ DC precursors expressed several chemokine receptors, including CCR1 and CCR5, thus suggesting that the migratory responses to MIP-1α seen in Fig. 2 are indeed confined to this subset.

Immunohistochemistry using both mouse and rabbit Abs demonstrated strong in situ CCR6 expression by dendritic epidermal cells of normal human skin (Fig. 6 B; data not shown). In serial sections, these cells were weakly HLA-DR^+, and thus represent LCs in their nonactivated state

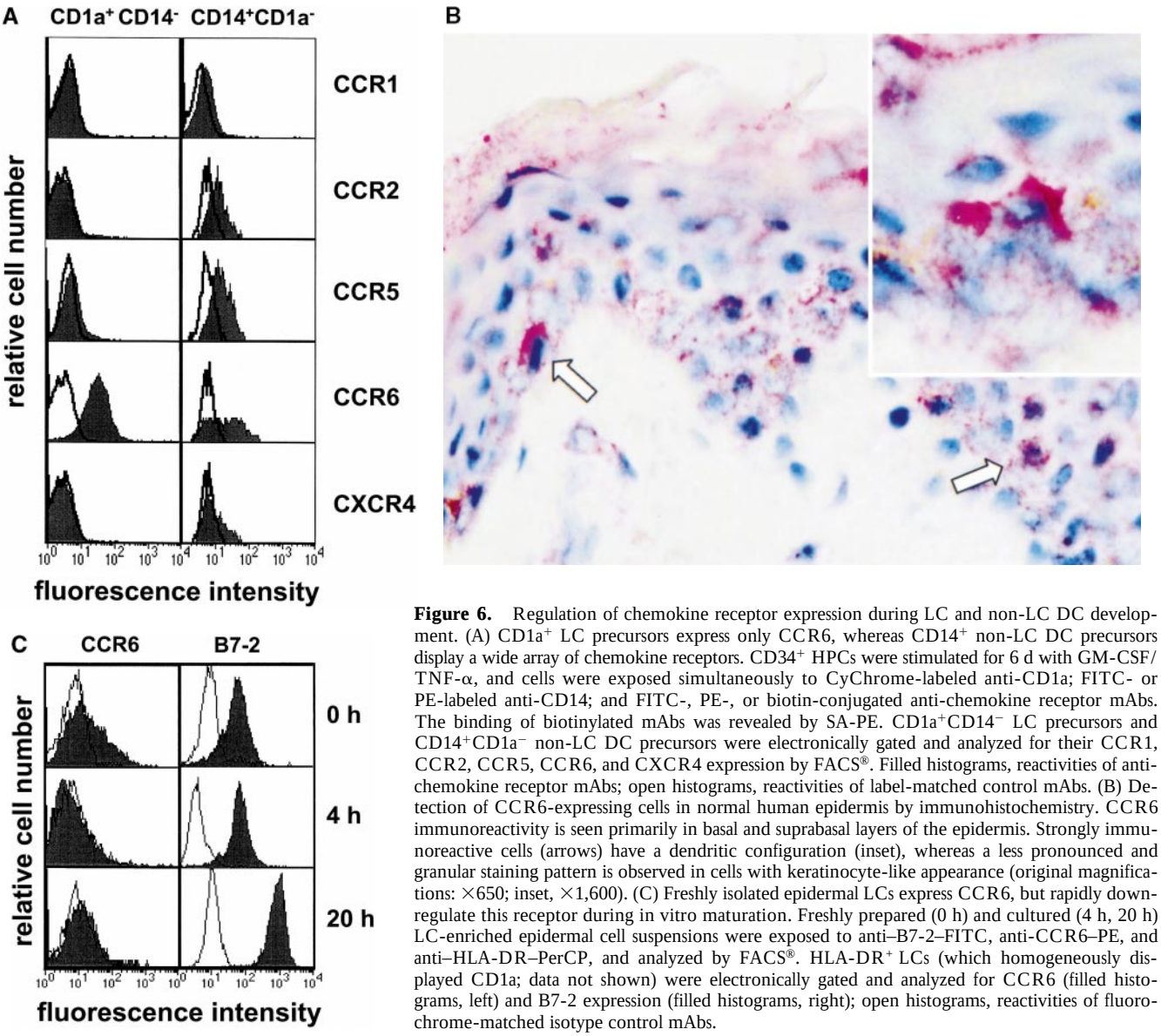

Figure 6. Regulation of chemokine receptor expression during LC and non-LC DC development. (A) $CD1a^+$ LC precursors express only CCR6, whereas $CD14^+$ non-LC DC precursors display a wide array of chemokine receptors. $CD34^+$ HPCs were stimulated for 6 d with GM-CSF/TNF-α, and cells were exposed simultaneously to CyChrome-labeled anti-CD1a; FITC- or PE-labeled anti-CD14; and FITC-, PE-, or biotin-conjugated anti-chemokine receptor mAbs. The binding of biotinylated mAbs was revealed by SA-PE. $CD1a^+CD14^-$ LC precursors and $CD14^+CD1a^-$ non-LC DC precursors were electronically gated and analyzed for their CCR1, CCR2, CCR5, CCR6, and CXCR4 expression by FACS®. Filled histograms, reactivities of anti-chemokine receptor mAbs; open histograms, reactivities of label-matched control mAbs. (B) Detection of CCR6-expressing cells in normal human epidermis by immunohistochemistry. CCR6 immunoreactivity is seen primarily in basal and suprabasal layers of the epidermis. Strongly immunoreactive cells (arrows) have a dendritic configuration (inset), whereas a less pronounced and granular staining pattern is observed in cells with keratinocyte-like appearance (original magnifications: ×650; inset, ×1,600). (C) Freshly isolated epidermal LCs express CCR6, but rapidly downregulate this receptor during in vitro maturation. Freshly prepared (0 h) and cultured (4 h, 20 h) LC-enriched epidermal cell suspensions were exposed to anti–B7-2–FITC, anti-CCR6–PE, and anti–HLA-DR–PerCP, and analyzed by FACS®. $HLA\text{-}DR^+$ LCs (which homogeneously displayed CD1a; data not shown) were electronically gated and analyzed for CCR6 (filled histograms, left) and B7-2 expression (filled histograms, right); open histograms, reactivities of fluorochrome-matched isotype control mAbs.

(data not shown). In most experiments we also observed a weak, albeit distinct, granular anti-CCR6 reactivity in keratinocytes of the Malpighian layer (Fig. 6 B). Our additional finding of CCR6 mRNA in purified keratinocytes (data not shown) is indicative of receptor synthesis by these cells. CCR6 surface expression by a major subset of freshly isolated $HLA\text{-}DR^+$ $CD1a^+$ LCs was also demonstrated by FACS® (Fig. 6 C). In vitro culture of these LCs under maturation-promoting conditions resulted in a rapid loss of anti-CCR6 surface immunoreactivity that even preceded the maturation-related upregulation of the costimulatory molecule B7-2 (Fig. 6 C). These data suggest that epidermal LCs, although $CCR6^+$ in their nascent state, downregulate this receptor during the process of in situ maturation. In correlation with these results and the maturation-dependent responses of LCs to either MIP-3α or MIP-3β (Figs. 1 and 4), we observed a complete loss of CCR6 mRNA production with continued synthesis of CCR7 mRNA during cytokine-mediated maturation of epidermal LCs (Fig. 5 C). Similarly to CCR6 mRNA, CCR2 transcripts disappeared during the in vitro maturation of epidermal LCs, whereas the expression of CXCR4 mRNA remained unchanged (Fig. 5 C). In conclusion, it appears that immature LCs ex vivo and those generated in vitro display a similar and restricted set of chemokine receptors, and that mature cells no longer produce chemokine receptor mRNAs, with the notable exception of CCR7 and CXCR4.

In view of data published previously by Zaitseva et al. (32), the apparent lack of CCR5 mRNA expression by epidermal LCs appears surprising. Although unlikely, it is conceivable that LCs express CCR5 mRNA at levels too low to be detected by our RT-PCR assay. It is important to note that the LC-purification strategy employed here strictly excluded $CD2^+$ and/or $CD3^+$ skin T cells that ex-

press CCR5 (data not shown). Moreover, using two different mAb clones and RT-PCR, we also failed to detect CCR5 protein and mRNA expression by in vitro–generated LCs (Fig. 5 A; data not shown), but could amplify CCR5-specific transcripts from day 6 cytokine-stimulated HPCs (Fig. 5 D) and from freshly isolated and cytokine-stimulated PB-DCs (Fig. 5 E; data not shown).

MIP-3α is the Prime Candidate for Recruiting LC Precursors into the Epidermis. To get information about the expression of chemokines in normal human skin and to correlate it with the chemokine receptor pattern of LC precursors, we performed immunohistochemistry and RT-PCR on frozen skin sections and FACS®-purified skin cells, respectively. Keratinocytes were found to express MIP-3α mRNA (Fig. 7 I); accordingly, MIP-3α immunoreactivity was seen in the basal and suprabasal layers of the epidermis (Fig. 7 A). RT-PCR revealed no MIP-3β mRNA in isolated keratinocytes (Fig. 7 I). Together with our finding of only sparse and focal epidermal MIP-3β immunoreactivity (not shown), this suggests that MIP-3β, unlike MIP-3α, is not constitutively produced in the epidermis. Conversely, we observed strongly MIP-3β–immunoreactive cells throughout the dermis (Fig. 7 D). SDF-1α immunoreactivity was seen in the epidermis but, in contrast to MIP-3α, its expression was strictly confined to the basal keratinocyte layer (Fig. 7 C). As shown in Fig. 7 E, normal human epidermis is devoid of MCP-1 immunoreactivity, an observation that finds support in a previous publication (33). Also, no MIP-1α, MIP-1β, or RANTES immunoreactivity was seen in normal epidermal keratinocytes (data not shown).

Thus, it appears that two chemokines, MIP-3α and SDF-1α, are produced constitutively by human keratinocytes, and therefore could both be involved in LC homing to the epidermis. Our findings that SDF-1α does not attract LC precursors (Fig. 1 C) and that these cells also fail to express CXCR4 on their surface (Fig. 6 A) speak against a role of SDF-1α in LC homing. Since ex vivo–purified LCs express CCR2 transcripts (Fig. 5 B), one could argue that this receptor is involved in the attraction of LCs into the epidermis. This is unlikely because (a) resting keratinocytes do not express the CCR2 ligand MCP-1 at the protein level (33; Fig. 7 E), and (b) LC precursors do not express CCR2 on their surface (Fig. 6 A), and do not migrate in response to MCP-1 (Fig. 1 B). In this context, it is noteworthy that mice genetically manipulated to express MCP-1 in the epidermis have close to normal LC numbers while accumulating dermal DCs and macrophage-like cells (34).

In conclusion, among all the chemokine–chemokine receptor pairs studied, only MIP-3α–CCR6 fulfills the spatial and temporal expression, as well as function requirements, for a ligand–receptor pair responsible for LC homing to the epidermis. This is evidenced by (a) the constitutive expression of MIP-3α in normal human epidermis (Fig. 7, A and I); (b) the selective in vitro chemotactic responses of $CD1a^+$ LC precursors to MIP-3α (Figs. 1 A and 3 A); (c) the expression of CCR6 by in vitro–generated LC/LC precursors (Figs. 5 A and 6 A), by skin-derived LCs (Figs. 5 B and 6 C), and by LCs in situ (Fig. 6 B); (d) the absence of CCR6 from non-LC DCs, e.g., PB-DCs (Fig. 5 E), mdDCs (17), and dermal DCs (data not shown); and (e) the rapid loss of CCR6 surface expression during LC maturation, as illustrated by a reverse regulation of CCR6 and B7-2 expression during LC culture (Fig. 6 C), and the lack of CCR6 expression by cytokine-matured epidermal LCs (Fig. 5 C).

MIP-3α, although absent from spleen and bone marrow, is also expressed in appendix, thymus, and tonsils as well as in fetal liver and lung (35–39). Curiously, in tonsils (18), skin (this study), and perhaps also in the other organs containing epithelial cells, MIP-3α is expressed constitutively by ectodermal rather than bone marrow–derived cells. Because keratinocytes produce MIP-3α (Fig. 7, A and I), and at the same time apparently also express CCR6 (Fig. 6 B; data not shown), it is possible that, in addition to driving LC homing, this chemokine plays a previously unrecognized autocrine role in keratinocyte homeostasis.

If MIP-3α is expressed in several different organs, why do immature LCs appear only in stratified epithelia? It is conceivable that additional factors, and not MIP-3α expression alone, determine whether LC precursors can populate a given organ. A prerequisite for homing into the epidermis is the emigration of LC precursors from the circulation, which, by analogy with other leukocytes, is likely to be mediated by a cascade of discrete multistep interactions with ECs (40). Organ-specific differential expression of endothelial adhesion molecules may provide an important additional source for the selectivity of LC homing into skin. The multistep adhesion paradigm may also explain how the lack of expression of leukocyte adhesion molecules, e.g., cutaneous lymphocyte-associated antigen (CLA), may be responsible for the fact that not all CCR6-bearing blood leukocytes (28) can enter the skin in response to MIP-3α.

We argued above that MIP-3α is ideally positioned to guide the migration of LC precursors into the epidermis, but can it also drive their emigration from blood? To do this, MIP-3α would have to be associated with dermal ECs and appear on their luminal surface (41, 42). This could be achieved either by EC binding and transcytosis of keratinocyte-derived MIP-3α, as has been demonstrated previously for IL-8 and RANTES (42), or by ECs themselves producing MIP-3α, as was shown for other chemokines (43). Postcapillary and small venular ECs in normal human skin display MIP-3α immunoreactivity (Fig. 7 H), and isolated DMECS produce MIP-3α mRNA (Fig. 7 I), showing that, in addition to keratinocytes, dermal ECs also produce this chemokine under normal conditions. The lack of MIP-3α mRNA in HUVECs (Fig. 7 I) underlines the site-specific differences among ECs. Cumulatively, these findings suggest that, in addition to navigating LCs towards the epidermis, MIP-3α may be the chemokine responsible for the transendothelial migration of LC precursors.

Additionally, the immunohistochemical studies revealed MIP-3α and MIP-3β immunoreactivity to be associated with the ECs of afferent lymphatics (Fig. 7, F and G). This observation is in line with our previous in situ binding studies, which demonstrated the presence of saturable, broad specificity binding sites for CC (MCP-1, MCP-3, RANTES)

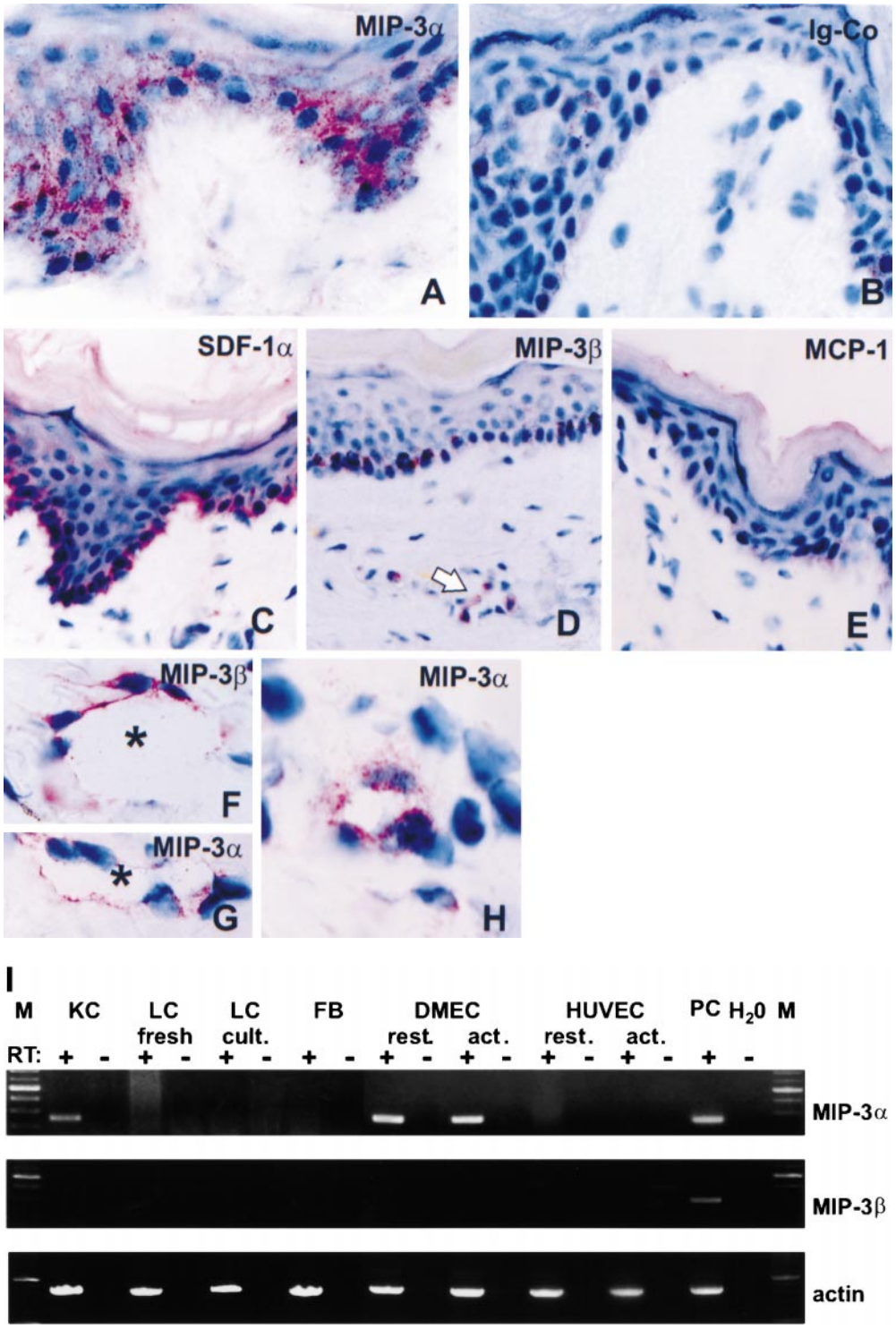

Figure 7. Chemokine expression in normal human skin. (A) Pronounced MIP-3α immunostaining of basal and suprabasal keratinocytes. (B) Rabbit Ig control staining (Ig-Co). (C) Only basal keratinocytes display SDF-1α immunoreactivity. (D) No MIP-3β immunoreactivity is seen in the epidermis, but scattered dermal cells are stained (arrow). (E) Neither the epidermis nor the dermis reacts with anti–MCP-1 Abs. (F and G) ECs lining afferent lymphatics display MIP-3β and MIP-3α immunoreactivity (asterisks in F and G, respectively). (H) MIP-3α–positive ECs lining a postcapillary venule (original magnifications: A and B, ×1,400; C, D, and E, ×900; F and G, ×2,100; H, ×3,000). (I) RT-PCR analysis of MIP-3α and MIP-3β mRNA expression by keratinocytes (KC); freshly isolated (LC fresh) as well as ex vivo–matured epidermal LCs (LC cult.); fibroblasts (FB); DMECs; and HUVECs, the latter two with and without IFN-γ stimulation. RT, reverse transcription of mRNA; M, molecular size markers; PC, positive control for MIP-3α and MIP-3β mRNA expression (i.e., reverse-transcribed mRNA from tonsillar extracts, reference 14). PCR with β-actin–specific primers is shown (bottom; control for the cDNA content of individual samples).

but not CXC chemokines on the lymphatic ECs in human dermis (44). Additionally, SLC immunoreactivity was shown to be associated with lymphatic vessels (45). The functional significance of chemokine binding to this microanatomical location is not yet clear. It is possible that chemokines immobilized on lymphatic ECs facilitate the entry of LCs into the lymphatics or, alternatively, promote their movement within the lymphatic channels toward the draining lymph node. In both cases, the primary role is likely to be played by CCR7 ligands, since LCs at this stage of their maturation downregulate CCR6 expression.

In this study, we show that LCs display a chemokine response pattern that is much narrower than perhaps anticipated. Thus, the restricted set of chemokine receptors expressed by constitutively trafficking LCs stands in striking contrast to the very broad chemokine receptor repertoire of DCs that

appear under inflammatory conditions (5, 10, 13, 31; this study). These findings suggest a scenario where the differential behavior of two ontogenetically different DC lineages is encoded by their differential expression of chemokine receptors. One cell type, the LC, follows only one tissue-derived constitutive signal, MIP-3α, and is remarkably ignorant to inflammation-related chemokine stimuli. As a result, it resides in the skin and plays a role in the homeostatic host defense. Another cell type, exemplified by the PB-DC, lacks CCR6 but displays a broad repertoire of chemokine receptors and, consequently, can home to any inflammatory site where it perpetuates or modulates the inflammatory tissue response. It also appears that the ultimate step in the DC odyssey, i.e., their migration into draining lymph nodes, follows one pattern common to all DC subtypes: LCs, non-LC DCs (this study; 18, 45), and monocyte-derived DCs (10, 13, 19, 20) start to express CCR7 and respond to MIP-3β upon receipt of maturation-promoting stimuli. This chemokine, and probably also the alternative CCR7 ligand SLC (22, 45), may guide DCs into T cell areas of draining lymph nodes.

The skilled technical help of Erni Schwarzinger is gratefully acknowledged. We wish to thank Dr. Joshua Farber (National Institutes of Health, Bethesda, MD), Dr. Tom Schall (Chemocentrix, Mountain View, CA), and Dr. Matthias Schmudt (University of Innsbruck Medical School, Innsbruck, Austria) for donating reagents, Dr. Marion Gröger (Department of Dermatology, University of Vienna Medical School) for providing DMECs and HUVECs, and Dr. Peter Wolf Husslein (Department of Obstetrics and Gynecology, University of Vienna Medical School) for the supply of CB samples.

This work was supported in part by grants from the Austrian Ministry of Science and Transportation, and from Novartis Ltd., Basel, Switzerland. A.-S. Charbonnier was supported in part by grants from the Fondation René Touraine (France) and the Austrian Science Foundation (S06702-MED).

Address correspondence to Dieter Maurer, Division of Immunology, Allergy and Infectious Diseases, Department of Dermatology, University of Vienna Medical School, Waehringer Guertel 18-20, A-1090 Vienna, Austria. Telephone: 43-1-40-400-7769; Fax: 43-1-403-1900; E-mail: dieter.maurer@akh-wien.ac.at

Submitted: 23 July 1999 Revised: 20 September 1999 Accepted: 28 September 1999

References

1. Steinman, R.M. 1991. The dendritic cell system and its role in immunogenicity. *Annu. Rev. Immunol*. 9:271–296.
2. Banchereau, J., and R.M. Steinman. 1998. Dendritic cells and the control of immunity. *Nature*. 392:245–252.
3. Stingl, G., D. Maurer, C. Hauser, and K. Wolff. 1999. The epidermis: an immunologic microenvironment. *In* Dermatology in General Medicine. Vol. 1. I.M. Freedberg, A.Z. Eisen, K. Wolff, K.F. Austen, L.A. Goldsmith, S.I. Katz, and T.B. Fitzpatrick, editors. McGraw-Hill, New York, NY. 343–370.
4. Maurer, D., and G. Stingl. 1999. Dendritic cells in the context of skin immunity. *In* Dendritic Cells. M.T. Lotze, and A.W. Thompson, editors. Academic Press, San Diego, CA. 111–122.
5. Robert, C., R.C. Fuhlbrigge, J.D. Kieffer, S. Ayehunie, R.O. Hynes, G. Cheng, S. Grabbe, U.H. von Andrian, and T.S. Kupper. 1999. Interaction of dendritic cells with skin endothelium: A new perspective of immunosurveillance. *J. Exp. Med*. 189:627–636.
6. Randolph, G.J., S. Beaulieu, S. Lebecque, R.M. Steinman, and W.A. Muller. 1998. Differentiation of monocytes into dendritic cells in a model of transendothelial trafficking. *Science*. 282:480–483.
7. Wollenberg, A., S. Kraft, D. Hanau, and T. Bieber. 1996. Immunomorphological and ultrastructural characterization of Langerhans cells and a novel, inflammatory dendritic epidermal cell (IDEC) population in lesional skin of atopic eczema. *J. Invest. Dermatol*. 106:446–453.
8. Baggiolini, M. 1998. Chemokines and leukocyte traffic. *Nature*. 392:565–568.
9. Rollins, B.J. 1997. Chemokines. *Blood*. 90:909–928.
10. Sallusto, F., P. Schaerli, P. Loetscher, C. Schaniel, D. Lenig, C.R. Mackay, S. Qin, and A. Lanzavecchia. 1998. Rapid and coordinated switch in chemokine receptor expression during dendritic cell maturation. *Eur. J. Immunol*. 28:2760–2769.
11. Sozzani, S., F. Sallusto, W. Luini, D. Zhou, L. Piemonti, P. Allavena, J. Van Damme, S. Valitutti, A. Lanzavecchia, and A. Mantovani. 1995. Migration of dendritic cells in response to formyl peptides, C5a, and a distinct set of chemokines. *J. Immunol*. 155:3292–3295.
12. Sozzani, S., W. Luini, A. Borate, N. Polentarutti, D. Zhou, L. Piemonti, G. D'Amico, C.A. Power, T.N.C. Wells, M. Gobbi, et al. 1997. Receptor expression and responsiveness of human dendritic cells to a defined set of CC and CXC chemokines. *J. Immunol*. 159:1993–2000.
13. Lin, C.L., R.M. Suri, R.A. Rahdon, J.M. Austyn, and J.A. Roake. 1998. Dendritic cell chemotaxis and transendothelial migration are induced by distinct chemokines and are regulated on maturation. *Eur. J. Immunol*. 28:4114–4122.
14. Rubbert, A., C. Combadiere, M. Ostrowski, J. Arthos, M. Dybul, E. Machado, M.A. Cohn, J.A. Hoxie, P.M. Murphy, A.S. Fauci, and D. Weissman. 1998. Dendritic cells express multiple chemokine receptors used as coreceptors for HIV entry. *J. Immunol*. 160:3933–3941.

15. Godiska, R., D. Chantry, C.J. Raport, S. Sozzani, P. Allavena, D. Leviten, A. Mantovani, and P.W. Gray. 1997. Human macrophage-derived chemokine (MDC), a novel chemoattractant for monocytes, monocyte-derived dendritic cells, and natural killer cells. *J. Exp. Med*. 185:1595–1604.
16. Delgado, E., V. Finkel, M. Baggiolini, C.R. Mackay, R.M. Steinman, and A. Granelli-Piperno. 1998. Mature dendritic cells respond to SDF-1, but not to several β-chemokines. *Immunobiology*. 198:490–500.
17. Greaves, D.R., W. Wang, D.J. Dairaghi, M.C. Dieu, B. de Saint-Vis, K. Franz-Bacon, D. Rossi, C. Caux, T. McClanahan, S. Gordon, et al. 1997. CCR6, a CC chemokine receptor that interacts with macrophage inflammatory protein 3α and is highly expressed in human dendritic cells. *J. Exp. Med*. 186:837–844.
18. Dieu, M.C., B. Vanbervliet, A. Vicari, J.M. Bridon, E. Oldham, S. Ait-Yahia, F. Briere, A. Zlotnik, S. Lebecque, and C. Caux. 1998. Selective recruitment of immature and mature dendritic cells by distinct chemokines expressed in different anatomic sites. *J. Exp. Med*. 188:373–386.
19. Sozzani, S., P. Allavena, G. D'Amico, W. Luini, G. Bianchi, M. Kataura, T. Imai, O. Yoshie, R. Bonecchi, and A. Mantovani. 1998. Differential regulation of chemokine receptors during dendritic cell maturation: a model for their trafficking properties. *J. Immunol*. 161:1083–1086.
20. Yanagihara, S., E. Komura, J. Nagafune, H. Watarai, and Y. Yamaguchi. 1998. EBI1/CCR7 is a new member of dendritic cell chemokine receptor that is up-regulated upon maturation. *J. Immunol*. 161:3096–3102.
21. Sallusto, F., and A. Lanzavecchia. 1999. Mobilizing dendritic cells for tolerance, priming, and chronic inflammation. *J. Exp. Med*. 189:611–614.
22. Gunn, M.D., S. Kyuwa, C. Tam, T. Kakiuchi, A. Matsuzawa, L.T. Williams, and H. Nakano. 1999. Mice lacking expression of secondary lymphoid organ chemokine have defects in lymphocyte homing and dendritic cell localization. *J. Exp. Med*. 189:451–460.
23. O'Doherty, U., M. Peng, S. Gezelter, W.J. Swiggard, M. Betjes, N. Bhardwaj, and R.M. Steinman. 1994. Human blood contains two subsets of dendritic cells, one immunologically mature, and the other immature. *Immunology*. 82:487–493.
24. Kohrgruber, N., N. Halanek, M. Gröger, D. Winter, K. Rappersberger, M. Schmitt-Egenolf, G. Stingl, and D. Maurer. 1999. Survival, maturation, and function of $CD11c^-$ and $CD11c^+$ peripheral blood dendritic cells are differentially regulated by cytokines. *J. Immunol*. 163:3250–3259.
25. Petzelbauer, P., J.R. Bender, J. Wison, and J.S. Pober. 1993. Heterogeneity of dermal microvascular endothelial cell antigen expression and cytokine responsiveness in situ and in cell culture. *J. Immunol*. 151:5062–5072.
26. Bleul, C.C., M. Farzan, H. Choe, C. Parolin, I. Clark-Lewis, J. Sodroski, and T.A. Springer. 1996. The lymphocyte chemoattractant SDF-1 is a ligand for LESTR/fusin and blocks HIV-1 entry. *Nature*. 382:829–832.
27. Rot, A., L.E. Henderson, T.D. Copeland, and E.J. Leonard. 1987. A new series of ligands for the human formyl peptide receptor. Tetrapeptides with high chemotactic potency and efficacy. *Proc. Natl. Acad. Sci. USA*. 88:7967–7971.
28. Liao, F., R.L. Rabin, C.S. Smith, G. Sharma, T.B. Nutman, and J.M. Farber. 1999. CC chemokine receptor 6 is expressed on diverse memory subsets of T cells and determines responsiveness to macrophage inflammatory protein 3 alpha. *J. Immunol*. 162:186–194.
29. Caux, C., B. Vanbervliet, C. Massacrier, C. Dezutter-Dambuyant, B. de Saint-Vis, C. Jacquet, K. Yoneda, S. Imamura, D. Schmitt, and J. Banchereau. 1996. $CD34^+$ hematopoietic progenitors from human cord blood differentiate along two independent dendritic cell pathways in response to GM-CSF+TNFα. *J. Exp. Med*. 184:695–706.
30. Kim, C.H., and H.E. Broxmeyer. 1998. In vitro behavior of hematopoietic progenitor cells under the influence of chemoattractants: stromal cell-derived factor-1, steel factor, and bone marrow environment. *Blood*. 91:100–110.
31. Ayehunie, S., E.A. Garcia-Zepeda, J.A. Hoxie, R. Horuk, T.S. Kupper, A.D. Luster, and R.M. Ruprecht. 1997. Human immunodeficiency virus-1 entry into purified blood dendritic cells through CC and CXC chemokine coreceptors. *Blood*. 90:1379–1386.
32. Zaitseva, M., A. Blauvelt, S. Lee, C.K. Lapham, V. Klaus-Kovtun, H. Mostowski, J. Manischewitz, and H. Golding. 1997. Expression and function of CCR5 and CXCR4 on human Langerhans cells and macrophages: implication for HIV primary infection. *Nat. Med*. 3:1369–1375.
33. Barker, J.N., M.L. Jones, C.L. Swenson, V. Sarma, R.S. Mitra, P.A. Ward, K.J. Johnson, J.C. Fantone, V.M. Dixit, and B.J. Nickoloff. 1991. Monocyte chemotaxis and activating factor production by keratinocytes in response to IFN-gamma. *J. Immunol*. 146:1192–1197.
34. Nakamura, K., I.R. Williams, and T.S. Kupper. 1995. Keratinocyte-derived monocyte chemoattractant protein 1 (MCP-1): analysis in a transgenic model demonstrates MCP-1 can recruit dendritic and Langerhans cells to skin. *J. Invest. Dermatol*. 105:635–643.
35. Hieshima, K., T. Imai, G. Opdenakker, J. Van Damme, J. Kusuda, H. Tei, Y. Sakaki, K. Takatsuki, R. Miura, O. Yoshie, and H. Nomiyama. 1997. Molecular cloning of a novel human CC chemokine liver and activation-regulated chemokine (LARC) expressed in liver. Chemotactic activity for lymphocytes and gene localization on chromosome 2. *J. Biol. Chem*. 272:5846–5853.
36. Rossi, D.L., A.P. Vicari, K. Franz-Bacon, T.K. McClanahan, and A. Zlotnik. 1997. Identification through bioinformatics of two new macrophage proinflammatory human chemokines: MIP-3α and MIP-3β. *J. Immunol*. 158:1033–1036.
37. Hromas, R., P.W. Gray, D. Chantry, R. Godiska, M. Krathwohl, K. Fife, G.I. Bell, J. Takeda, S. Aronica, M. Gordon, et al. 1997. Cloning and characterization of exodus, a novel β-chemokine. *Blood*. 89:3315–3322.
38. Baba, M., T. Imai, M. Nishimura, M. Kakizaki, S. Takagi, K. Hieshima, H. Nomiyama, and O. Yoshie. 1997. Identification of CCR6, the specific receptor for a novel lymphocyte-directed CC chemokine LARC. *J. Biol. Chem*. 272:14893–14898.
39. Varona, R., A. Zaballos, J. Gutierrez, P. Martin, F. Roncal, J.P. Albar, C. Ardavin, and G. Marquez. 1998. Molecular cloning, functional characterization and mRNA expression analysis of the murine chemokine receptor CCR6 and its specific ligand MIP-3 alpha. *FEBS Lett*. 440:188–194.
40. Butcher, E.C., and L.J. Picker. 1996. Lymphocyte homing and homeostasis. *Science*. 272:60–66.
41. Rot, A. 1992. Endothelial cell binding of NAP-1/IL-8: role in neutrophil emigration. *Immunol. Today*. 13:291–294.
42. Middleton, J., S. Neil, J. Wintle, I. Clark-Lewis, H. Moore, C. Lam, M. Auer, E. Hub, and A. Rot. 1997. Transcytosis and surface presentation of IL-8 by venular endothelial cells. *Cell*. 91:385–395.
43. Wolff, B., A. Burns, J. Middleton, and A. Rot. 1998. Endothelial cell "memory" of inflammatory stimulation: human venular endothelial cells store interleukin 8 in Weibel-Palade

bodies. *J. Exp. Med*. 188:1757–1762.
44. Hub, E., and A. Rot. 1998. In situ binding of Rantes, MCP-1, MCP-3, and MIP-1α to cells in human skin. *Am. J. Pathol*. 152:749–757.
45. Saeki, H., A.M. Moore, M.J. Brown, and S.T. Hwang. 1999. Secondary lymphoid-tissue chemokine (SLC) and CC chemokine receptor 7 (CCR7) participate in the emigration pathway of mature dendritic cells from the skin to regional lymph nodes. *J. Immunol*. 162:2472–2475.
46. Dragic, T., V. Litwin, G.P. Allaway, S.R. Martin, Y. Huang, K.A. Nagashima, C. Cayanan, P.J. Maddon, R.A. Koup, J.P. Moore, and W.A. Paxton. 1996. HIV-1 entry into $CD4^+$ cells is mediated by the chemokine receptor CC-CKR-5. *Nature*. 381:667–673.